JOURNAL OF SPACECRAFT AND ROCKETS
Vol. 39, No. 6, November–December 2002

Realizing "2001: A Space Odyssey": Piloted Spherical Torus Nuclear Fusion Propulsion

Craig H. Williams,* Leonard A. Dudzinski,† Stanley K. Borowski,‡ and Albert J. Juhasz§
NASA John H. Glenn Research Center at Lewis Field, Cleveland, Ohio 44135

A conceptual vehicle design enabling fast, piloted outer solar system travel was created, predicated on a small aspect ratio spherical torus nuclear fusion reactor. The mission requirements were satisfied by the vehicle concept, which could deliver a 172-t crew payload from Earth to Jupiter rendezvous in 118 days, with an initial mass in low Earth orbit of 1690 t. Engineering conceptual design, analysis, and assessment was performed on all major systems, including artificial gravity payload, central truss, nuclear fusion reactor, power conversion, magnetic nozzle, fast wave plasma heating, tankage, fuel pellet injector, startup/restart fission reactor and battery bank, refrigeration, reaction control, mission design, and space operations.

Nomenclature

C3 = hyperbolic excess velocity squared, km^2/s^2
I_{sp} = specific impulse
N_e = electron number density
n = neutron
T_e = electron temperature
T_L = low-temperature sink
α = specific power
γ = gamma radiation
η_J = overall jet efficiency

Subscripts

e = electric
th = thermal

Introduction

THE impetus for this effort was to guide advanced space propulsion research to enable a long-range goal of human expansion throughout the solar system. Nuclear fusion space propulsion has been shown to be capable of enabling order-of-magnitude improvements in space transportation capability and has been discussed in a recent series of analytic studies.[1–7] In this work, results have shown that for piloted, outer solar system missions expected within the 21st century, adequate payload mass fraction (5–15%) and multimonth trip times would require I_{sp} and α of 20,000–50,000 lbf s/lbm and 5–50 kW/kg, respectively.[1,4–6]

Based in part on the results of previous studies,[4,8] the closed magnetic fusion confinement concept, a small aspect ratio spherical torus, was chosen as the basis for this vehicle concept. The high-power density achievable in a spherical torus, improved confinement, spin polarization of fuel, and density and temperature profile peaking provided advantages in its application toward space propulsion.

State-of-the-art fusion confinement systems intended for terrestrial power and scientific research, along with experimental results, were used as the basis for extrapolation to what could be technologically available to a human presence solar system wide of the not too distant future, 30 years from now. Most of the propulsion vehicle system engineering data were derived from expendable launch vehicle operational experience and conceptual nuclear thermal rocket design studies. Only limited fusion space propulsion system data exist beyond what was accomplished since the termination of the 20-year nuclear fusion program in 1978. In 2001, the similarities between the spacecraft in the highly acclaimed motion picture "2001: A Space Odyssey" and this vehicle concept have inspired the authors to honor the movie's creators by christening this vehicle concept the *Discovery II*.

Mission Requirements

The reference missions selected were to destinations in the outer solar system, where dozens of scientifically interesting worlds will compel human exploration in the future. The missions were to provide a logical progression to the considerable mission planning that has been conducted over the years on more near-term, inner solar system destinations, that is, the moon and Mars. Outer solar system distances are ~1–2 orders of magnitude greater than those of the inner solar system and, thus, will require revolutionary improvements in propulsion.

The *Discovery II* was to be able to perform a rendezvous (one-way) mission to either Jupiter or Saturn, piloted by a crew of 6–12, with a >5% payload mass fraction and a trip time of less than one year. The specific destinations were Jupiter's moon Europa and Saturn's moon Titan. These two moons were selected because of their demanding performance requirements, scientifically interesting possibility of life on their surfaces requiring human presence for investigation, dominant size among other moons, expected abundance of hydrogen for propulsion application, and abundance of fusion fuels D_2 and ^3He in their planet's atmosphere. Based primarily on existing human-to-Mars mission studies, a minimum crew size of six was chosen. The piloted nature of the mission also drove the requirement for relatively fast trip times. The one-year maximum was somewhat arbitrary, but was representative of long-duration human experience in low Earth orbit and consistent with current Mars mission studies.

Vehicle Overview

Figures 1 and 2 illustrate the overall layout of the *Discovery II*. The rotating crew payload was forward of the propulsion system. It was linked to the central truss through a fixed central hub, which

Presented as Paper 2001-3805 at the 37th Joint Propulsion Conference, Salt Lake City, UT, 8–11 July 2001; received 31 October 2001; revision received 22 May 2002; accepted for publication 22 May 2002.

*Aerospace Engineer, Space Transportation Project Office, M.S. 86-8, 21000 Brookpark Road; lvcraig@grc.nasa.gov. Associate Fellow AIAA.

†Aerospace Engineer, Systems Engineering Division, M.S. 86-15, 21000 Brookpark Road; Leonard.A.Dudzinski@grc.nasa.gov. Member AIAA.

‡Advanced Concepts Program Manager, Space Transportation Project Office, M.S. 86-8, 21000 Brookpark Road; Stanley.K.Borowski@grc.nasa.gov. Associate Fellow AIAA.

§Senior Research Engineer, Power and On-Board Propulsion Technology Division, M.S. 301-3, 21000 Brookpark Road; Albert.J.Juhasz@grc.nasa.gov. Associate Fellow AIAA.

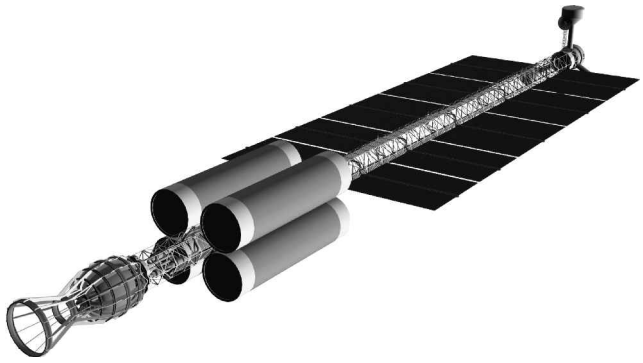

Fig. 1 ***Discovery II*** **vehicle concept.**

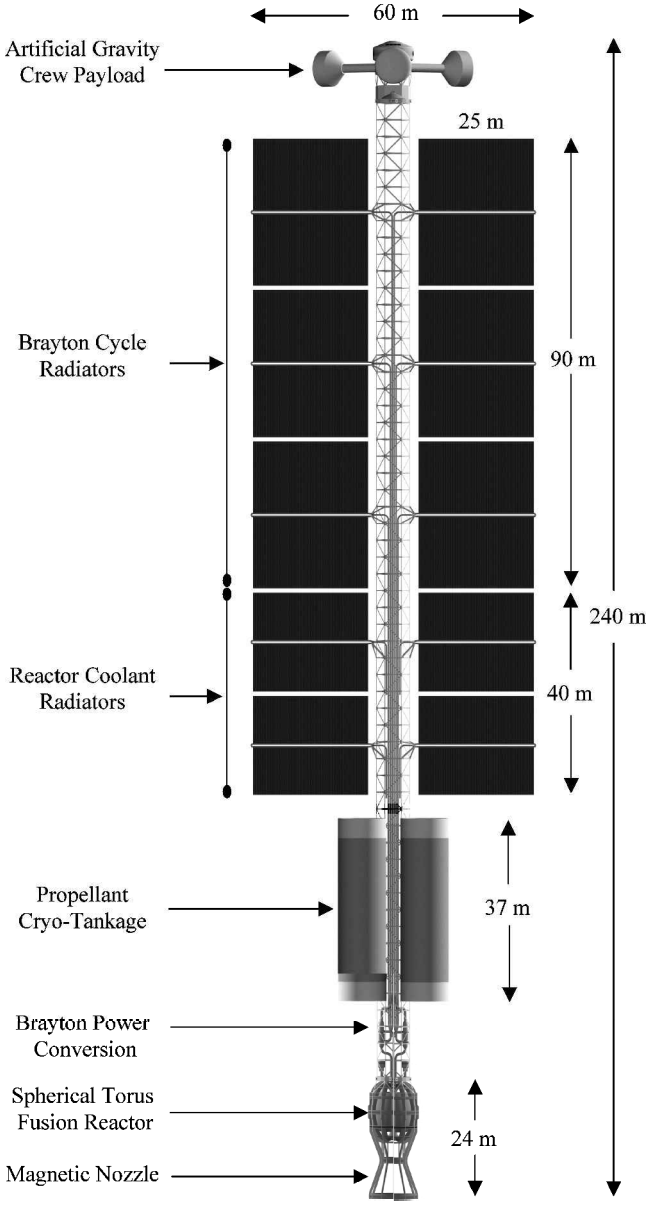

Fig. 2 ***Discovery II*** **vehicle concept system layout.**

also attached to the avionics suite and truss booms supporting the communication antennas. The forward central truss supported the two, coplanar, low- and high-temperature heat rejecting radiators. Four slush hydrogen propellant tanks were mounted along the outside of the midcentral truss. Within the midcentral truss was the D^3He fuel tank and refrigeration system for all propellant/fuel tankage. Throughout the central truss were also various data, power, coolant, and propellant lines. Within the aft central truss was the Brayton power conversion system. Also within the aft central truss were the power management and distribution system, the refrigeration system, the start/restart reactor, and battery bank. Running the entire length of the central truss was the fuel pellet injection system. Aft of the central truss were the spherical torus nuclear fusion reactor, fast wave heating, and the magnetic nozzle. The overall vehicle length was 240 m. The longest deployed system dimensions were the 203-m central truss and the 25-m heat rejection (radiator) systems. The maximum stowed diameter for any individual system, however, was limited to 10 m to fit within the envisioned payload fairing, facilitating launch and on-orbit assembly. The fully tanked initial mass in low Earth orbit (IMLEO) was 1690 t.

Table 1 Vehicle mass property summary

System	Subsystem	Mass, t	Mass, t
Payload			172
	Structure	38	
	Shielding	69	
	Crew systems	25	
	Weight growth contingency	40	
Structure			646
	Central truss	6	
	Fusion reactor	310	
	Magnetic nozzle/divertor	6	
	Reaction control	16	
	Power conversion	30	
	Coolant system	11	
	Fast wave plasma heating	5	
	Propellant cryo-tankage	88	
	Refrigeration	2	
	Fuel tankage and injector	6	
	Startup/restart fission reactor	10	
	Battery bank	5	
	Avionics and communication	2	
	Weight growth contingency	149	
D^3He fuel			11
Hydrogen propellant			861
	Main impulse	807	
	Reaction control	20	
	Flight performance reserve	8	
	Residuals/losses	26	
IMLEO			1690

Table 1 illustrates the mass property summary for the design reference mission's fully loaded stack. The payload mass was 172 t and consisted of useful payload only. The fuel mass was 11 t of D^3He for the nuclear fusion reactor. The slush hydrogen propellant mass was 861 t, was primarily for main impulse and did not include system or tankage mass. The total structure mass was 646 t and referred to all mass required to operate the propulsion system, including weight growth contingency.

Mission Analysis

Fusion propulsion systems are expected to operate at high enough I_{sp} and α to produce accelerations greater than the local acceleration due to solar gravity at Earth's orbit (0.6 mg) (Refs. 1 and 4). The normally thought of conics of minimum energy trajectories followed by today's chemical systems degenerate into nearly straight line, radial transfers at these high acceleration levels with continuous thrust. As will be shown, with an initial thrust to weight of 1.68 mg, the *Discovery II*'s trajectory was reasonably close to that of a radial transfer. Figure 3 is a heliocentric view of an optimized, integrated trajectory from Earth to Saturn.

Table 2 contains the overall performance analysis results for the *Discovery II*. All vehicle mass properties were fixed for both missions The Earth-to-Jupiter rendezvous mission thrust was 6250 lbf, had an I_{sp} of 35,435 lbf s/lbm, and had a propellant flow rate of 0.079 kg/s. The Earth-to-Saturn rendezvous mission thrust was 4690 lbf, I_{sp} of 47,205 lbf s/lbm, and had a propellant flow rate of 0.044 kg/s. Rendezvous missions were integrated for the optimal departure dates. The payload modules for the Jupiter and Saturn missions were both 172 t. The 118-day (~4-month) trip time to Jupiter and 212-day (~7-month) trip time to Saturn were rapid compared to those of representative alternate concepts, where similar rendezvous

Table 2 Mission analysis results

Parameter	Jupiter	Saturn
Mission type	Rendezvous	Rendezvous
Travel distance, AU	4.70	9.57
Specific power, kW/kg	8.62	~Same
Specific impulse, lbf s/lbm	35,435	47,205
Payload mass, t	172	Same
IMLEO, t	1,690	1,699
Trip time, days	118	212
Jet power, MW	4,830	Same
Jet efficiency	0.8	Same
Thrust, lbf	6,250	4,690
Total flow rate, kg/s	0.080	0.045
Exhaust velocity/char velocity	0.92	~Same
Initial thrust/mass, mg	1.68	1.25

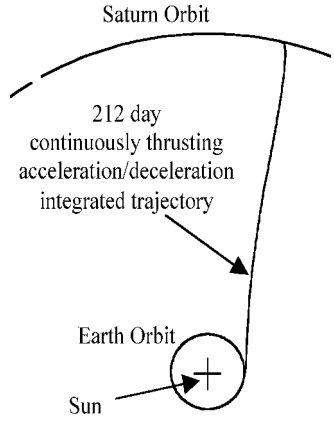

Fig. 3 Integrated Earth to Saturn trajectory.

mission trip times using chemical or even nuclear thermal propulsion would be measured in years. These results suggest that the *Discovery II* could accomplish fast interplanetary trip times with significant payloads over broad launch opportunities.

Space Operations

The large-vehicle mass-driven IMLEO represented a fundamental obstacle to viable space operations. The *Discovery II*'s IMLEO was ~17 times what could be delivered to low Earth orbit (LEO) by a launch system in the Space Shuttle System class of ~100 t (without Orbiter).[9] A new heavy lift launch vehicle (HLLV) would be required. Sized for the greatest single payload masses and volumes, the HLLV throw-weight capability was envisioned to be ~250 t to LEO. Even with this capability, seven HLLVs would be required for the initial mission, and four HLLVs for subsequent missions (propellant resupply). A preliminary manifest was prepared to ensure that each HLLV launch could accommodate the mass and dimensions of aggregate payloads. Table 3 shows LEO assembly characteristics.

On-orbit assembly would be a necessity for this concept. Individual systems were configured to maximize simpler rendezvous and docking techniques. However, even with a new HLLV, serious concerns remain regarding multimonth launch availability and cost. If fusion concepts prove to be as massive as the current design suggests, HLLV operations could prove development lethal for fusion propulsion.

Rendezvous missions were selected as the modus operandi due to their enabling of dramatic reductions in propellant requirements, vehicle size, and improved performance compared to carrying sufficient propellant for round-trip missions.[1,6] The implied requirement of a planetary refueling capability [in situ resource utilization (ISRU), with considerable infrastructure] is of great concern but is consistent with a solar-system-class transportation system regularly journeying to and between large outer planets with atmospheres and moons rich in H_2, D_2, and ^{3}He. Sources of available propellant near high departure/arrival orbits, such as water ice at the lunar poles, minor moons, outermost major moons, and even asteroids, would greatly facilitate refueling without entering into deep gravity wells, provided the facilities could be established and maintained at

Table 3 Assembly characteristics

Parameter	Design value
Number of HLLV launches	
Vehicle	3
Propellants	4
Assembly sequence	
Flight 1	Truss, auxiliary power, RCS, etc.
Flight 2	Fusion reactor, nozzle, etc.
Flight 3	Payload, etc.
Flights 4–7	Propellant
HLLV throw weight, t	251
HLLV payload fairing	
Diameter, m	10
Length, m	37
Assembly orbit	
Altitude, nmile	260 circular
Inclination, deg	28.5
Assembly method	Rendezvous, dock
Crew transport	Dedicated vehicle
IMLEO, t	1690

Table 4 Space operation characteristics

Parameter	Design value
Mission type	Rendezvous
Maximum range, AU	~50
Maximum duration, month	12
Departure/arrival planetary orbits, C3	~0
Infrastructure required per planet	
Crew transport: low orbit to C3 ~ 0	1
Propellant/deuterium ISRU plant	1
Propellant tankage	4
Atmospheric ^{3}He miner	1
Number of propellant resupply launches	4
Propellant/deuterium ISRU source	Major moon
Vehicle staging or drop tanks	No
Vehicle life	Reusable

a sufficiently low cost. ^{3}He would be acquired through ISRU by either collecting solar wind deposited or scavenging major planetary atmospheric deposits, which would alleviate the supply issue.

The *Discovery II* was, thus, designed for interplanetary cruise only. Table 4 illustrates selected space operation characteristics. A high-altitude, subparabolic orbit (C3 ~ 0 km^2/s^2) space basing obviated the need for multiweek spiral escapes and captures at its origin and destination and also lessened the operation limits, particularly near populated areas such as a space station. It was envisioned that steady-state operation (following initial assembly in LEO and predeployment of space infrastructure) would consist of direct flights to the outer planets, with only refueling operations taking place before return (Fig. 4).

Payload

Overview

The most difficult obstacles to long-duration human interplanetary travel are the detrimental effects of weightlessness and radiation on the human body. These two areas will have significant impacts on human payload design studies and are the main reasons for the *Discovery II's* new payload system.

The crew modules were new designs, with subsystems scaled from a recent Mars study.[10] The designs were compared to International Space Station (ISS) modules. This permitted a reasonable check of the mass properties for subsystems by way of habitable volume-to-mass scaling. A significant difference when compared to ISS was the use of graphite–epoxy (GrEp) IM7/977-2 in lieu of aluminum to reduce mass and the generation of secondary radiation products from solar and deep-space sources. All of the modules were sized on HLLV throw weight and corresponding payload fairing dimensions.

The crew payload comprised three rotating laboratory/habitation (Lab/Hab) modules attached to the fixed central hub via three connecting tunnels (Fig. 5). The Lab/Hab modules were the primary laboratory and habitation facilities for the crew and were where most of the astronauts' time would be spent in a constant 0.2-*g*

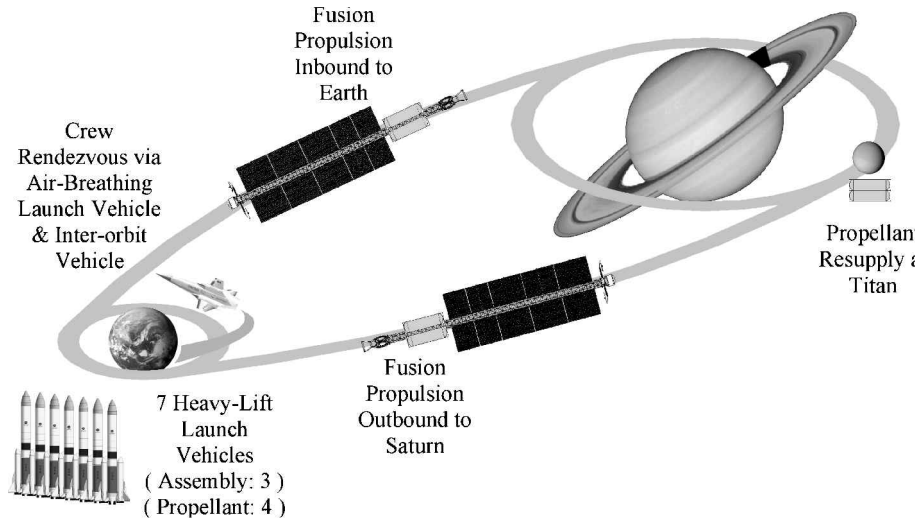

Fig. 4 Space operation scenario.

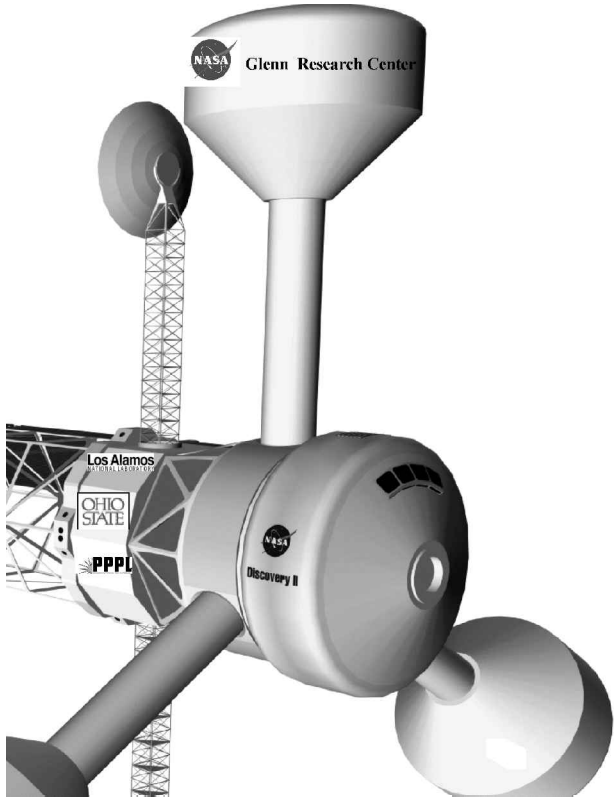

Fig. 5 Artificial gravity crew payload.

artificial gravity environment. The Lab/Hab modules were 7.5 m in diameter, of sufficient height to permit a two-story layout, and each contained crew accommodations for at least four crewmembers, as well as scientific, healthcare, and recreation equipment. They also had independent life-support, vehicle status, thermal, power, communication, extravehicular activity (EVA), and data systems. Consumables included sufficient air, water, and food for up to one year.[10] For safety, each module had two physically separate means of crew egress. For the Lab/Hab modules, this meant the addition of an airlock outfitted with space suits.

The central hub served as the fixed interface for both the crew transport vehicle docking port (fore) and the fusion propulsion system (aft). These parts were inertially fixed, with the middle serving as the rotating link with the three tunnels that provided access to the three Lab/Habs. The central hub was also heavily shielded to serve as the storm shelter for ambient high-radiation events. The total habitable volume was 872 m^3, of which the three Lab/Hab modules provided 495 m^3. The total mass of the payload was 172 t, which included a 30% weight growth contingency (Table 5).

Table 5 Payload mass properties

System	Subsystem	Mass, t	Mass, t
Structure			38
	Lab/Hab modules (3)	7	
	Central hub	4	
	Tunnels (3)	2	
	Airlocks (3)	1	
	Structural beef-up	3	
	Power management	2	
	Avionics	1	
	Life support	12	
	Thermal control	4	
	Rotation start/stop RCS	2	
	Payload adapter	~0	
Shielding			69
	Storm shelter	47	
	Nominal radiation	13	
	Thermal	1	
	Micrometeoroid	1	
	Containment hull	7	
Crew systems			25
	Accommodations	8	
	Consumables	10	
	Crew/suits	3	
	EVA equipment	2	
	Science	2	
Weight growth contingency			40
Total			172

Artificial Gravity

The detrimental effects of weightlessness on the human body have been observed for decades. Bone decalcification and muscle atrophy represent leading threats to the health and effectiveness of astronauts on interplanetary missions.[11] The artificial gravity concept adopted for the *Discovery II* was a derivative of a previously created and published concept.[12]

The amount of artificial gravity required for crew health has been the subject of considerable study, though it is thought that a minimum of 0.2 *g* (~lunar gravity) might be sufficient to at least facilitate locomotion. *Discovery II's* 17-m rotation arm and 3.25-rpm rotation rate produced an artificial gravity level of 0.2 *g* at the Lab/Hab floor, which satisfied the suggested guidelines for maximum walking-to-rim speed ratio and radial gravity gradient (Table 6).

Shielding from Ambient Radiation

Multimonth trip times through interplanetary space have the concomitant danger of exposure to lethal doses of ambient radiation

unless the crew payload is adequately shielded. The most serious concerns lie with galactic cosmic rays (GCR) and solar proton flares. GCRs are stripped atomic nuclei at GeV energies that originate in interstellar space and penetrate our sun's magnetosphere.[13] Flares are high-energy protons ejected from the sun throughout its 11-year solar cycle.

The ambient radiation shielding design for the *Discovery II* was adopted from a recent Mars mission design study.[13] The nominal radiation shield for the *Discovery II* consisted of a layer of liquid water surrounding all modules, enveloped by a GrEp containment hull wrapped by 50.8-mm (2-in.) multilayer insulation (MLI) thermal protection and 0.5-mm aluminum micrometeoroid shielding. Water was chosen due to the low atomic mass of hydrogen and the resultant low generation of secondary radiation products. For nominal shielding on all habitable parts of the payload except the storm shelter 2 g of H_2O/cm^2 was used. The water shielding provided radiation dose equivalent (REM) ~55-rem/year 5-cm depth dose equivalent for GCR (at solar minimum), which slightly exceeded the LEO guideline (see Table 6).[14] The storm shelter had robust shielding (20 g of H_2O/cm^2), which provided an ~30-rem/year 5-cm depth dose equivalent for GCR (at solar minimum), but was achieved at a considerable mass penalty of ~47 t (Table 5).

Table 6 Payload system characteristics

Parameter	Design value
Nominal crew size	6–12
Consumables, months	12
Number of habitable modules	7
Module structural material	GrEp
Lab/Hab, central hub diameter, m	7.5
Lab/Hab height (two story), m	5.6
Storm shelter height, m	7.8
Total habitable volume, m^3	872
Artificial gravity, g	0.2
Rotation rate, rpm	3.25
Rotation arm, m	17
Maximum walking-to-rim speed ratio	0.17
Radial gravity gradient, mg/m	12
Nominal GCR maximum dose, rem/yr	~55
Storm shelter GCR maximum dose, rem/yr	~30
Radiation shielding (nominal), cm H_2O	2
Radiation shielding(storm shelter), cm H_2O	20
MLI thermal shielding, mm	50.8
Micrometeoroid shielding, mm	0.5
Power consumption (steady state), kW_e	30
Mass, t	172

Fusion Reactor

Overview

Unlike today's terrestrial reactors that must be safely isolated from the biosphere, a largely skeletal design was used for the *Discovery II*. Smaller in size than current research reactors, the design philosophy was to minimize mass, maximize useful charged power out, and facilitate direct radiation of waste power to space without a containment vessel. An ignited plasma operating mode was chosen, as well as a high bootstrap current, to minimize the recirculating power fraction required and the concomitant conversion system mass for generating injection power. It was thought that a continuously thrusting propulsion system would be better served by this mode of reactor operation, where charged transport power was used exclusively for propulsion purposes. A small-major-radius (2.48-m) and small-aspect-ratio (2.0) reactor geometry was chosen to minimize size and mass. The scaling for toroidal beta favored elongated (3:1), compact devices with large plasma currents (~66 MA) and moderately large centerline magnetic fields (8.9 T). These magnetic field requirements led to very large toroidal field (TF) coil currents (9.2 MA). There were 12 TF coils used to generate the toroidal magnetic field; seven poloidal field (PF) coils were used to provide plasma stability. Existing materials were used with occasional extrapolations of physical properties, evaluated at operating temperatures.

Figure 6 illustrates the radial build, including an upper half of one TF D-shape coil and its inboard assembly. Beginning with the reactor centerline and working outboard, an annulus along the centerline provided a flow channel for the slush hydrogen propellant. A vacuum gap separated it from a titanium alloy compression structure

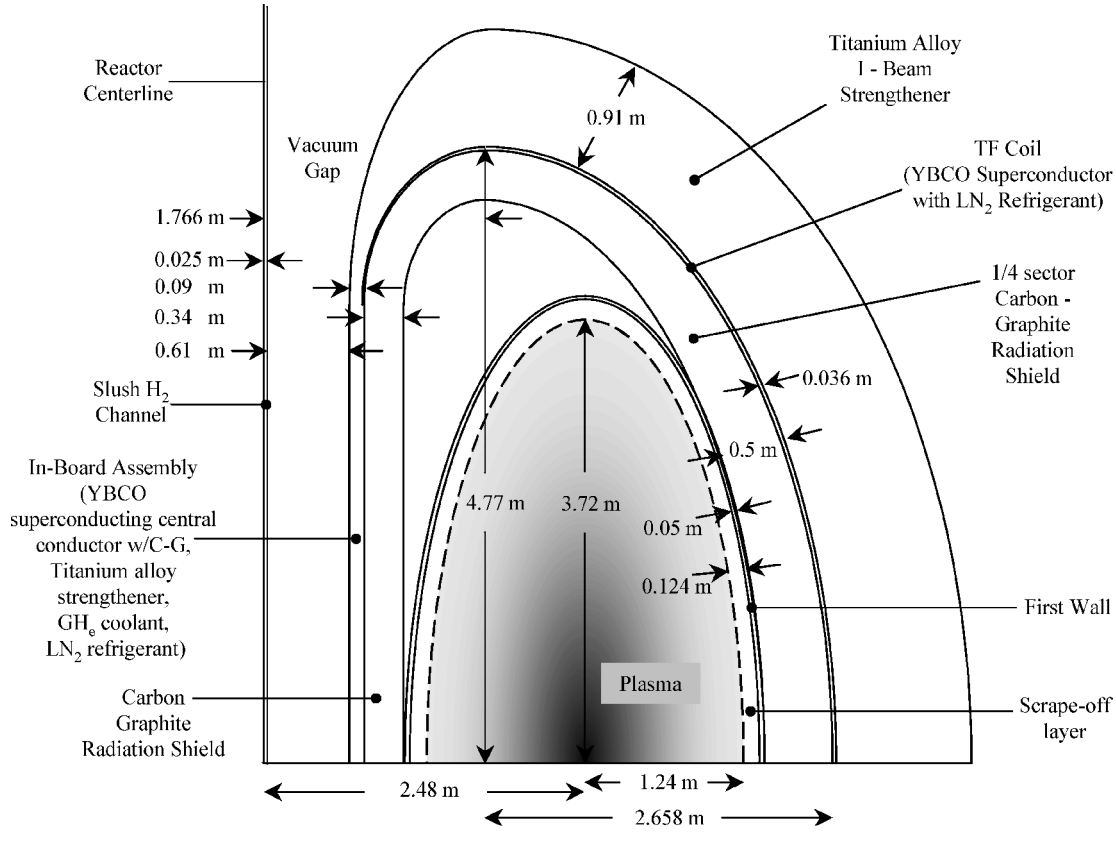

Fig. 6 Fusion reactor radial build.

that provided support for the current-induced coil loads. A high-temperature superconductor coating on a composite structure supported the large current that generated the toroidal magnetic field. Several coolant and refrigeration channels provided heat transfer for absorbed radiation and maintained cryogenic temperatures. A carbon composite/W_2B_5 shield attenuated most of the radiation that was transmitted through the first wall. A double hull, carbon composite first wall was coated with optical grade beryllium on the plasma-facing surface. A scrapeoff layer of ash was assumed to be 10% of the 1.24-m minor radius. The outboard structures were similar. A slightly thicker, one-quarter-sector radiation shield was used to shadow the TF coil from the core. A coolant channel for heat transfer was positioned behind the shield. The TF coil was jacketed with refrigerant to maintain cryogenic conditions. A large titanium alloy I-beam strengthener was used to counter the tension loads generated by the TF coil currents. Further outboard (not shown) were the PF coils and supporting equipment (including support for the high harmonic fast wave heating system).

Plasma Modeling and Characteristics

Modeling of the plasma conditions was performed through a one-dimensional plasma power balance computer program.[15] When peaked temperature and number density profiles were pursued within the core of a plasma, a relatively small fusion-producing region was established, satisfying Lawson and ignition criteria without necessitating large beta throughout the plasma. The lower temperature and number density outer regions would contribute to a volume-averaged beta value within magnetohydrodynamic stability limits. This approach was tremendously attractive for space propulsion applications, where compact size (and, thus, reduced mass) is of paramount importance. Charged particle and neutron power density, including DD side reactions, were integrated as functions of number density and radius (along with temperature dependent reactivities). Other primary reactor characteristics such as plasma current, magnetic field, confinement time scaling, etc., were determined while satisfying constraints such as critical beta and plasma power balance. Volume-averaged quantities such as transport power and radiation loss were used to determine initial available charged power for propulsion and available waste power for conversion to auxiliary electrical power, respectively. Plasma transport loss power, which included convection and conduction loss, represented the primary source of fusion reaction charged products for propulsion application and, thus, the quantity to be maximized.

D^3He (1:1 ratio) was chosen as the reactor fuel to maximize the charged transport power output and minimize neutron output power fraction. It was decided that in the time frame of this concept, reactor operation at a plasma temperature of 50 keV would represent only an incremental technological challenge over that of a DT-based concept. D^3He fuel with a spin vector polarized parallel to the magnetic field was used to capitalize on the up to 50% enhancement in fusion reactivity cross section,[16] greatly improving the charged output power fraction.

Table 7 illustrates selected reactor and plasma characteristics. No energy confinement time-scaling law exists based on experimental data for an ignited, steady-state thermonuclear device. However, an attempt was made to calibrate the reactor's operating characteristics with known total energy confinement time relations. A time of 0.552 s was in good agreement with the 1992 International Thermonuclear Experimental Reactor H-mode scaling law (0.565 s) (Ref. 17).

Power Generation and Utilization

Figure 7 illustrates the fusion power output and utilization. Of the 7895 MW of fusion power produced, 96% was in the form of charged particles with the remainder in (largely 2.45 MeV) neutrons. More than three-fourths of the power out of the reactor (6037 MW) was charged transport power (D and He ions, protons, and electrons), used solely for direct propulsion via the magnetic nozzle system. Synchrotron power (535 MW) was either

Table 7 Fusion reactor characteristics

Parameter	Design value
Major radius, m	2.48
Minor radius, m	1.24
Aspect ratio	2.0
Elongation	3.0
Plasma volume, m^3	225.8
Safety factor, edge	2.50
Safety factor, axis	2.08
Fuel ion density, $10^{20}/m^3$	5.0
Electron density, $10^{20}/m^3$	7.5
Plasma temperature, keV	50
Volume-averaged beta	0.318
Confinement time, s	0.552
Average neutron wall load, MW/m^2	1.03
Average radiation wall load, MW/m^2	5.20
Ignition margin	1.235
Toroidal magnetic field (centerline), T	8.9
Maximum magnetic field (coil surface), T	32.3
Gain factor	73.1
Plasma current, MA	66.22
Bootstrap current fraction (overdriven)	1.16
Wall reflectivity (effective)	0.98
Number density profile shape factor	1.0
Temperature profile shape factor	2.0

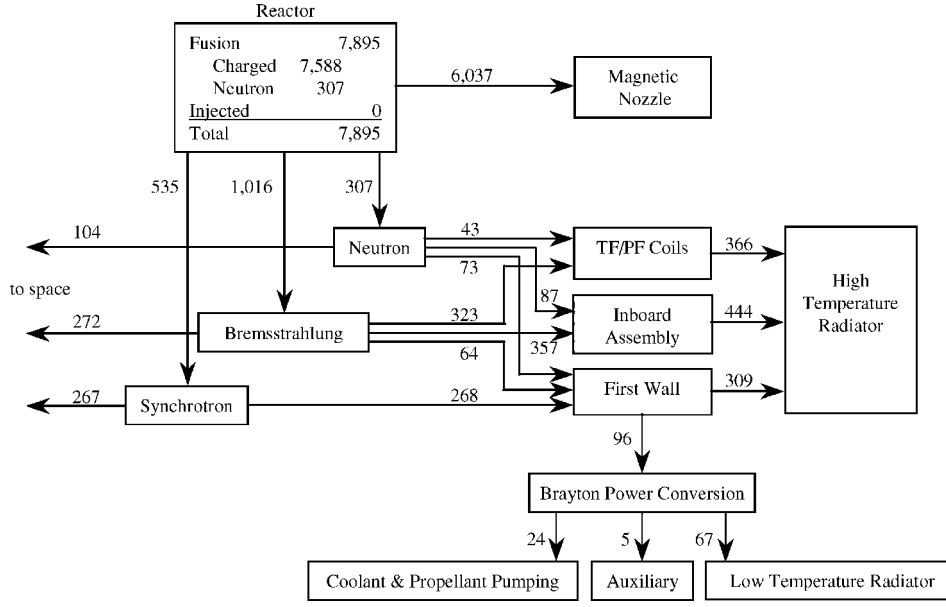

Fig. 7 Fusion power (megawatts) output and utilization.

Table 8 Auxiliary power usage [nominal (fusion) and startup (fission)]

System	Nominal, MW_e	Startup, MW_e
Electron cyclotron resonance heating	0	1
TF/PF magnetic nozzle refrigeration	3.95	0.39
Fuel injector	0.507	0.102
Battery recharge	0.16	0.125
Communications	0.2	Same
Propellant/fuel tankage refrigeration	0.133	Same
Payload	0.03	Same
Avionics	0.02	Same
Total	5	2

absorbed by the first wall or reflected out the divertor channel to space. Much of the Bremsstrahlung (1016 MW) and neutron radiation (307 MW) was absorbed throughout the reactor. Most of the heat generated by absorbed radiation (1119 MW) was transferred through a fan-circulated, gaseous helium (GHe) coolant system to a high-temperature radiator. The remaining heat from absorbed radiation (96 MW) was converted to electrical power for onboard use (~29 MW). No steady-state injection power was necessary due to the ignited, overdriven bootstrap current operation of the reactor system. The gain factor (fusion power/input power) based on the 108 MW of high harmonic fast wave startup heating was ~73.

Electrical power requirements were largely for the motor/fan-circulated GHe coolant system for the reactor (24 MW). The remaining power was consumed by propellant pumping and other auxiliary usage. Table 8 summarizes the nominal auxiliary power usage provided by the fusion reactor (5 MW_e) and startup/emergency restart power usage provided by the fission reactor (2 MW_e).

Radiation and Shielding Assessment

All radiation that did not pass directly to space was absorbed by the first wall and shield structures, converted to heat, and transferred by the GHe coolant. For the inboard assembly, opacity, high-temperature operation, and low density were needed for shielding the central superconductor from all Bremstrahlung and neutron radiation. Carbon–graphite was chosen to attenuate the inboard-bound neutrons, whereas the refractory tungsten boride (W_2B_5) was used to coat the shield's inboard side to absorb completely all Bremstrahlung radiation transmitted through the first wall. A small amount of the inboard assembly-bound residual neutron power, ~88 and ~45 kW, was absorbed by the superconducting magnets and its carbon–graphite (C–G) composite substrate structure, respectively. This heat was captured and rejected by the liquid nitrogen (LN_2) refrigeration system at 64 K.

TF/PF Coils

A 12-TF coil magnet and 7-PF coil magnet configuration was used. The coils' cross-sectional area was 75% $YBa_2Cu_3O_7$ (YBCO) jacketed by an LN_2 refrigerant, followed by an aluminum lithium casing. A summary of selected TF coil magnet parameters is given in Table 9. YBCO was chosen for its extremely high critical current density at moderate to large external magnetic fields, even at temperatures as high as 77 K (Ref. 18). Recent thin-film experiments using a chemical vapor deposition process have demonstrated critical current densities as great as 3000 MA/m^2 at ~65 K and magnetic fields of ~2 T (Ref. 19). In addition, irradiation experiments have measured enhancements in critical current density of up to a factor of four, suggesting that densities of the order of 12,000 MA/m^2 might be achievable in monolithic structures in the time frame of the *Discovery II*.

The high current (9.2 MA) carried in the coils that produced the tension loads necessitated strengtheners made from the highest yield strength material suitable for low-temperature applications. The titanium alloy, Ti-6Al-4V, was selected for its high yield strength at cryogenic temperatures.[20] The Ti-6Al-4V cross section design chosen was that of a TF coil-shaped American Institute of Steel Construction W-36 shape I beam. The 12-TF coil mass was ~129 t (Table 10).

The outboard C–G radiation shield was a one-quarter-sector cylinder design so that TF coils would be protected from neutron (and Bremsstrahlung) radiation from within a 90-deg angle centered on the reactor central axis. This design minimized shield mass, while also permitting neutrons that were not impacting the coils to pass directly to space. A minimum 50-cm blanket thickness was recommended for D^3He fueled reactors.[21,22]

Table 9 TF coil characteristics

Parameter	Design value
Number of coils	12
Superconductor material	YBCO
Length (without central conductor or trans), m	12.13
Radius, cm	1.8
Hydraulic diameter (w/5:1 fin ratio), m	0.04
Cross-sectional area (superconductor), %	75
Cross-sectional area (refrigerant), %	20
Current per coil, MA	9.2
Current density, MA/m^2	12,000
Toroidal magnetic field (centerline), T	8.9
Maximum magnetic field (self at coil), T	32.3
Maximum magnetic field (external), T	1.6
Operating temperature, K	65
Refrigerant	LN_2
Fluence, $10^{23}/m^2$	2.25
Coil strengthener material	Ti-6Al-4V
Strengthener configuration (I-beam)	W-36
Maximum tensile stress (65 K), N/m^2	19×10^8
Section modulus, m^3	0.052
Force per unit length (midplane), N/m	3.22×10^7
Force per unit length (top), N/m	7.38×10^7
Maximum bending moment, Nm	1.08×10^8
Total mass of 12 TF coils, t	128.6

Table 10 Fusion reactor mass properties

Subsystem	Mass, t
First wall	14
TF coils (12)	129
PF coils (7) and cross bracing	77
Neutron and radiation shielding	90
Total	310

Heat Transfer

A GHe coolant system was created to transfer the remaining radiation (65% of total produced) that was thermalized to the heat rejection system (radiators) and power conversion system at high temperature. GHe was chosen so that it could be used directly as the working fluid for the Brayton power conversion equipment due to its chemical inertness. High-pressure (7.5-MPa) operation was required, however, due helium's low heat capacity. Three commingled coolant loops transferred ~92% of the 1215 MW_{th} of thermal heat from the first wall, inboard assembly, and TF/PF coils to the radiators. Only 96 MW_{th} was bled off of the loops and sent to the power conversion cycle.

The GHe coolant was sent to a lightweight carbon-carbon (C–C), parallel duct heat pipe radiator panel array. By the use of a planar configuration, the 4070-m^2 area radiator was arranged as eight panels, rejecting heat from both sides. Each panel was designed to accommodate HLLV packaging, deployment, and rigidity imposed constraints (Table 11).

The first wall loop transferred 405 MW_{th} (including 96 MW_{th} to the Brayton power conversion system) of primarily thermalized synchrotron radiation at low flow speed. The inboard assembly/central conductor loop transferred 444 MW_{th} of thermalized neutron and Bremsstrahlung power at high flow speed. The TF/PF coil loop transferred 366 MW_{th} of thermalized neutron and Bremsstrahlung power at very low flow speed. Table 12 summarizes the heat transfer data for all three coolant loops.

Magnetic Nozzle

The conversion of the reactor's transport power into directed thrust was accomplished in two steps by the magnetic nozzle. In the first step, the nozzle mixed high-enthalpy transport plasma from

the divertor with the injected hydrogen propellant to reduce the excessive temperature and increase total charged propellant mass flow. In the second step, it converted the propellant enthalpy into directed thrust by accelerating the flow through converging/diverging magnetic field lines. In addition, its magnetic field prevented the high-temperature plasma from coming into contact with the nozzle's coils and structural members that make up the thrust chamber. Thus, for a fully ionized flow, the lines of magnetic flux also served as the containment device, minimizing heat transfer loses and the need for an actively cooled structure.

Table 11 Coolant system characteristics

Parameter	Design value
Coolant	GHe
Pressure, MPa	7.5
Temperature (hot gas), K	1700
Temperature (cold gas), K	997
Mass flow rate, kg/s	306.4
Power transferred, MW_{th}	1119
Radiator type	C–C heatpipe
Average temperature, K	1325
Total area, m^2	4070
Motor type	Three-phase ac, 600 Hz
Fan efficiency, %	92
System pressure loss, %	3.5
Fan type	Axial, single stage
Fan speed, rpm	9000
Fan power, MW_e	23.6

Table 12 Heat transfer characteristics (reactor side)

Parameter	First wall	Inboard	TF/PF
Coolant	GHe	Same	Same
Pressure, MPa	7.5	Same	Same
Temperature (hot gas), K	1700	Same	Same
Temperature (cold gas), K	1000	Same	Same
Temperature (wall), K	1824	1912	1759
Mass flow rate, kg/s	111	122	100
Velocity, m/s	44.6	341.3	25.0
Mach number	0.02	0.16	0.01
Reynolds number	1.247×10^5	9.540×10^5	4.830×10^4
Nusselt number	238	1212	111
Heat trans coefficient, W/m^2 K	1804	9190	1224
Heat transferred, MW	309 + 96	444	366

The I_{sp} of 20,000–50,000 lbf s/lbm and corresponding α required for multimonth travel to the outer planets required ion reservoir temperatures of hundreds of electron volts. The too great temperature and too small number density plasma layers that entered from the reactor's divertor had to be adjusted before acceleration through the nozzle to produce the mission appropriate I_{sp}. The escaping reactor plasma's condition was adjusted through the addition, heating, and ionizing of slush hydrogen propellant for thrust augmentation. The thrust-augmented plasma then possessed the desired values of bulk temperature (thus, I_{sp}) and mass flow rate (thus, thrust to weight). The propellant was then injected into the reservoir along the nozzle centerline.

A cross section of a conceptual magnetic nozzle is illustrated in Fig. 8. The "reservoir" of the magnetic nozzle was somewhat analogous to a conventional liquid chemical rocket engine's combustion chamber. Adjacent to the reactor's divertor, it consisted of two small-radius superconducting coils of the same design and materials as the TF coils. Forming an "effective" 10-cm-radius solenoid, they provided the meridional magnetic field to confine the converging propellant and reactor plasma streams until their temperatures equilibrated. The reservoir was in large part a "virtual" chamber due to its mostly skeletal design, where magnetic field lines defined the flow boundary for charged particles passing through. The second small-radius coil also constituted the "throat" for the nozzle, where choked flow (sonic) conditions existed. An arbitrarily larger-radius third coil formed the downstream, diverging section and provided additional curvature to the magnetic field.

The required downstream conditions for the exiting flow ($\eta_J \alpha = 6.9$ kW/kg and $I_{sp} = 35{,}435$ lbf s/lbm for the Jupiter mission) were used to initiate the flow calculations. The required fuel entry conditions from the divertor were found by working back up through the nozzle. These conditions were required to match the transport power available from the reactor. A one-dimensional model found that the required plasma state at the reservoir was a temperature of 252 eV and a number density of $1.35 \times 10^{22}/m^3$ (an order of magnitude lower and two orders of magnitude greater than that at the reactor scrapeoff layer, respectively) (Fig. 8).

Theory development was initiated to guide certain critical aspects of a new experiment that supported the vehicle design effort. The theory development is focused on characterizing the necessary plasma conditions for efficient magnetic nozzle operation. Certain gradient-driven microinstabilities are expected to impact flow symmetry negatively and instigate microturbulent, time-dependent fluctuations in the electric and magnetic fields.[23] If sufficient mixing of plasma and the magnetic field took place, it could adversely impact

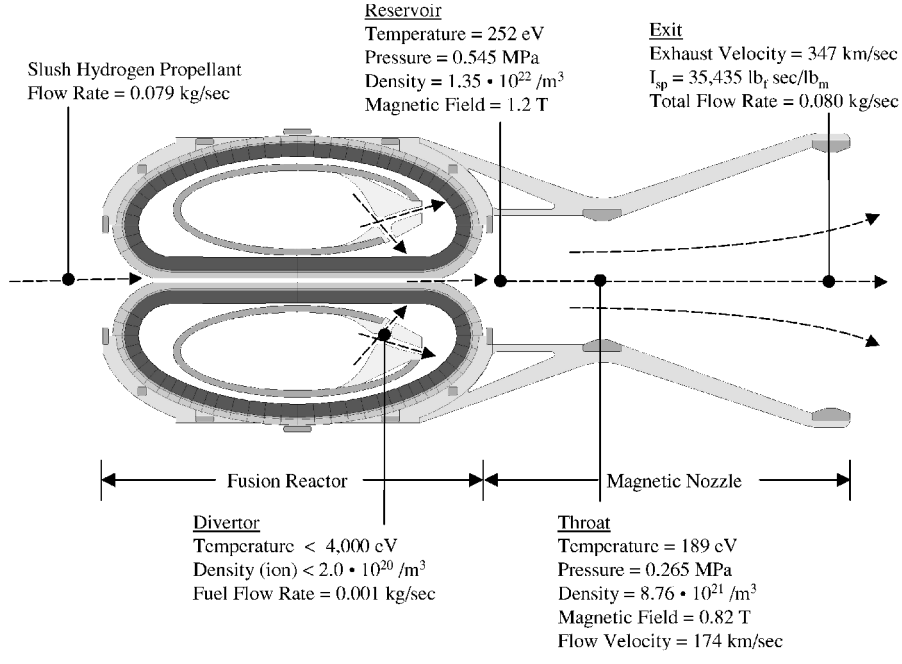

Fig. 8 Plasmas state conditions through magnetic nozzle.

the flow process, prompting inefficient detachment of plasma from field lines and, thus, significantly reducing propulsive thrust.

Magnetic nozzle experimentation applicable to fusion-class propulsion was recently initiated.[24] A small, proof-of-concept experiment is focused on providing key experimental data for gigawatt jet power level quasi-steady plasma flows and will measure fundamental physical parameters associated with generating and accelerating such plasmas. Of primary importance is obtaining experimental data with correct scaling of dimensionless variables to permit extrapolation into the regime of a full-scale *Discovery II*.

Reaction Control

A reaction control system (RCS) was designed to provide positive control of the vehicle's attitude and assist in main propulsion steering. Though the single-nozzle configuration would not be able to perform roll control, pitch and yaw was accomplished by selective, periodic reconfiguration of the nozzle's magnetic field geometry. A separate RCS was added that also provided for roll control. Because the *Discovery II* was significantly more massive than today's spacecraft and large quantities of electric power and hydrogen were available, the higher I_{sp} hydrogen fueled arcjet was used for the RCS.

An 8-MW/thruster design was based on a 30-kW hydrogen arcjet design[25] (Table 13). The RCS was composed of two units of four thrusters each. Each unit housed two thruster clusters 180 deg apart. Full control was provided with both units firing simultaneously. The aft unit was mounted on the aft end of the truss network, with the forward unit adjacent to the avionics suite.

Power Conversion

The primary function of the power conversion system was to utilize some of the Bremsstrahlung and neutron radiation by "thermalizing" this energy flux so that a fraction could be converted into electrical output power. A closed Brayton thermodynamic cycle [referred to as a closed-cycle gas turbine (CCGT)], was selected to accomplish the thermal-to-electric energy conversion. The CCGT was chosen on the basis of proven design and fabrication experience, a significant performance and reliability database, and the ability to use an inert gas as the working fluid.

The power flow design and cycle state points are illustrated in Fig. 9. The total thermal power supplied to the CCGT conversion system was 96 MW_{th} at 1700 K. Of this total thermal power, the gas-turbine power system converted 28.6 MW to electrical output power using a turboalternator. Approximately 67 MW_{th} was rejected into space by flat-plate heat pipe radiators that had a total radiating surface area of 10,000 m^2. The power conversion system was patterned after helium turbine designs for nuclear power plants advanced in Germany three decades ago.[26,27]

High Harmonic Fast Wave Heating

High harmonic fast wave (HHFW) heating is a promising method of noninductive plasma heating due to its potential for high heating efficiency (driven plasma current to injected power), high system efficiency (power output to power input), comparatively low system mass, and efficient volumetric packaging. The HHFW system was used for startup and to provide some control of the plasma current radial profile. The system was based partially on planning for the National Spherical Torus Experiment reactor[28] and a series of advanced fusion reactor conceptual designs.[29]

The HHFW system supplied power at high resonances of the ion cyclotron frequency. A projected heating efficiency of 0.1 A (driven)/W (injected) was used as well as the forecasted ~70% (power out to wall plug) system efficiency comparable to that for neutral beam systems.[29] A startup power of 108 MW was required from the HHFW to affect the overdriven current of 10.8 MA. The large peak power requirement (154 MW of HHFW) was the primary design driver for the startup battery bank.

Table 13 Reaction control characteristics

Parameter	Design value
Number of thruster units	2
Number of thruster clusters per unit	2
Number of thrusters per cluster	2
Number of thrusters (total)	8
Thruster type	Arcjet
Propellant	Hydrogen
Power per thruster, MW	8
Thrust, lbf	83
Specific impulse, lbf s/lbm	1480
Mass flow rate, kg/s	0.025
Efficiency, %	33.3
Roll maneuver	
Angular velocity, deg/min	1.24
Torque, N · m	2200
Firing time, s	30
Thrusters per maneuver	4
Battery bank supplied energy, MJ	960
Number of start/stop rolls per day	3
Total propellant mass, t	20
Total system dry mass (eight thrusters), t	16

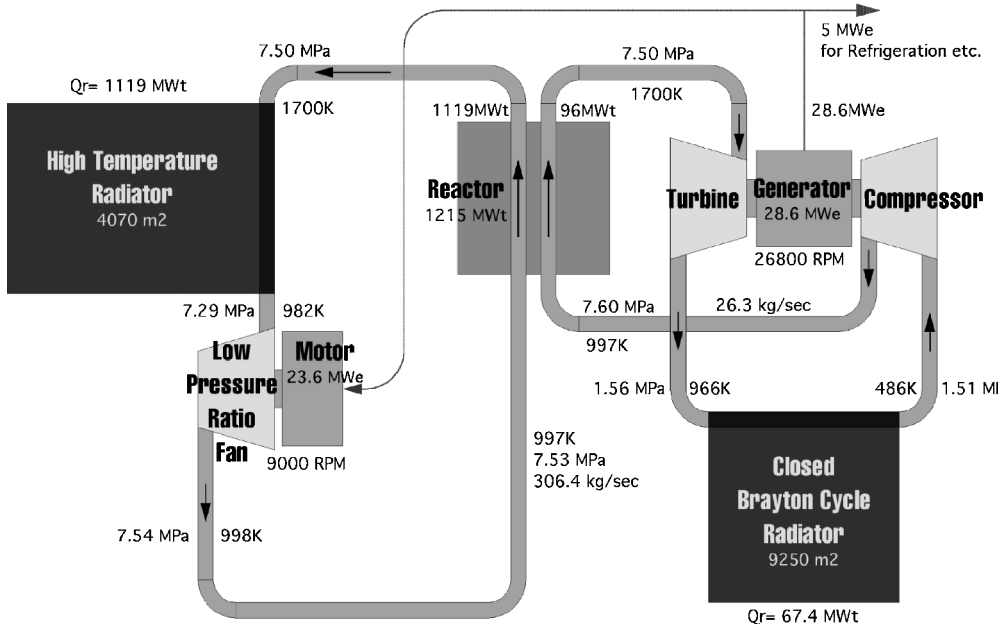

Fig. 9 Closed Brayton cycle power conversion and reactor coolant systems.

Table 14 Slush hydrogen propellant tankage characteristics

Parameter	Design value
Number of tanks	4
Delivery mode	HLLV (robotic)
Length (end to end), m	37
Length (barrel section), m	30
Diameter, m	10
Volume, m^3	2715
Pressure, psi	49.7
Ullage, %	2.5
Tank material	GrEp
Yield strength, ksi	80
Axial loading (maximum), *g*	4
Wall thickness (maximum), mm	6.1
Micrometeoroid shielding material	Aluminum
Multilayer insulation, cm	5
Operating temperature, K	14
Refrigerant	GHe
Refrigeration power, kW	29.5
Number of settling motors, 500 lbf	2
Number of attitude motors, 50 lbf	24
Flight performance reserve, %	1
Residuals and loses, %	3
Total tankable propellant, t	215
Dry mass, t	22

Table 15 Propellant tankage wet mass properties (single tank)

System	Subsystem	Mass, t	Mass, t
Propellant			215
	Main impulse	207	
	Flight perf. reserve	2	
	Residuals/losses	6	
Stage dry			22
Adapter			6
Contingency			8
GLOW, t			251

Propellant Cryotankage

The slush hydrogen propellant cryotankage was based on a preexisting conceptual design,[1] itself predicated on operational or previously designed conceptual liquid hydrogen propellant tanks.[30]

Tankage pressure and wall thickness were designed to accommodate a 4-*g* acceleration during Earth-to-orbit launch. A GrEp IM7/977-2 composite hydrogen tank material was used, and a 10-m diameter was maintained to not impact manufacturing and ground transportation limits significantly. The 3:1 aspect ratio (cylindrical barrel section length to diameter) yielded a total tank length of 37 m. The total tankable slush hydrogen propellant was calculated to be 215 t (Table 14). The subsystems were based primarily on two Centaur upper stage configurations flying on Atlas/Centaur and Titan IV/Centaur expendable launch vehicles.

Table 15 illustrates the mass summary for the fully loaded cryotankage in its Earth-to-orbit (ETO) launch configuration. The gross liftoff weight (GLOW) of a fully loaded cryotankage payload was 251 t, of which 207 t was slush hydrogen available for main impulse propulsion.

Refrigeration

Refrigeration was used to perform the initial cool down of vehicle systems before reactor ignition, remove any residual reactor heat not transferred by the GHe coolant during steady-state operation, and remove ambient (outer-space) heating. Considerable extrapolation was required from current space-qualified, long-life, mechanical cryocooler technology.[31] A gaseous helium Stirling cycle system[31] with a T_L of 3 K was used to refrigerate the solid/liquid D^3He fuel pellets. A gaseous helium Stirling cycle system[31] with a T_L of 10 K was used to refrigerate the slush hydrogen (SLH_2) propellant. An LN_2, multistage Joule–Thomson (J–T) system[31] with a T_L of 64.3 K was used to refrigerate the 65-K, 25 TF/PF/divertor/magnetic nozzle superconducting coils and the central conductor.

Table 16 Refrigeration characteristics

Parameter	TF/PF	SLH_2	D^3He
Cycle	J–T	Stirling	Stirling
Refrigerant	LN_2	GHe	GHe
COP, % Carnot	15	Same	Same
Temperature (hot), K	350	Same	Same
Temperature (cold), K	64.3	10	3
Temperature (wall), K	65	14	4
Heat transferred, W_{th}	133,350	519	13
Power required, kW_e	3,950	118	10
Mass, t	1.66	0.45	0.19

Table 17 Fuel injector characteristics

Parameter	Design value
Injector type	EM railgun
Length, m	185
Bore height, cm	3
Power (steady state), kW_e	507.5
Fueling rate (steady state), Hz	1
Pellet acceleration, *g*	27,580
Final velocity, km/s	10
Energy transfer efficiency, %	10
Injector mass, t	5
Power (startup), kW_e	101.5
Fueling rate (startup), Hz	0.2
Pellet material	Solid D, liquid ^3He
Pellet length (cube), cm	2.2
Pellet mass, *g*	1.015

The heat to be rejected was 519 W_{th} and 13 W_{th} from the propellant and fuel tankage, respectively, and was small compared to residual reactor steady-state heating that reached the YBCO superconductor and its C–G substrate (Table 16). Radiation analysis found that over 88- and 45-kW residual neutron heat was deposited in the YBCO central conductor and C–G substrate, respectively, and represented almost all of the refrigeration requirement. The electrical power required to operate the refrigeration systems assumed a coefficient of performance (COP) for the refrigerators was set at 15% of the Carnot COP.[32] There were 3950 kW_e of electrical power required to refrigerate the superconducting coils. The significantly smaller propellant and fuel tankage requirements were 118 and 10 kW_e, respectively (Table 16).

Fuel Injector and Tankage

The preponderance of fusion fuel injector design, fabrication, and operation experience has been with DT and DD. Very little effort, however, has be devoted to issues pertaining to injection of frozen D pellets encapsulating (liquid) ^3He.

The pellet injector design for the *Discovery II* was based on a promising concept for large pellets and high velocities: a plasma armature electromagnetic (EM) railgun. These devices have demonstrated accelerating 1-cm-sized polycarbonate pellets up to ~7 km/s, with energy transfer efficiencies of ~10% and constant accelerations up to $\sim 4.5 \times 10^6$ *g* (Refs. 33 and 34). They are, however, not reuseable at these demanding levels due to significant performance-driven erosion of the bore. Acceleration of frozen D pellets has been to only half of these velocities due to wall and electrode erosion.[33]

The pellet injector for the *Discovery II* operated at only 1% of acceleration levels of today's experimental devices; thus, a frequency capability of 1 Hz was assumed. The pellets were ~1 *g* each. A final pellet speed of 10 km/s was assumed to be required for adequate penetration to the plasma core. By the use of almost the entire length of the available central truss (185 m), a constant acceleration of 27,580 *g* was required. The steady-state power needed (assuming today's energy conversion efficiency of 10%) was 507 kW_e (Table 17).

To sustain a total fusion power of 7895 MW, D^3He fuel with a specific energy of 3.52×10^{14} J/kg must be consumed at a rate of ~22 mg/s. The average D^3He burn-up fraction was calculated to be only ~2.2%, requiring a fuel mass flow rate of ~1 g/s. At

Table 18 Fuel tankage characteristics

Parameter	Design value
Fuel tank length, m	4.1
Fuel tank diameter, m	6
Tank material	GrEp
Yield strength, ksi	80
Axial loading (maximum), g	4
Wall thickness (maximum), mm	6.1
Micrometeoroid shielding material	Aluminum
MLI, cm	5
Operating temperature, K	4
Refrigerant	GHe
Refrigeration power, kW_e	10.2
Fractional burn up, %	2.2
Flight performance reserve, %	1
Residuals and loses, %	3
Total tankable fuel, t	11
Dry mass, t	~1

this consumption rate, a 118-day trip to Jupiter required 11 t of D^3He (~6.7 t of ^3He). Tankage mass for the solid/liquid D^3He fuel pellets was estimated by scaling from the SLH_2 propellant tankage (Table 18).

Startup/Restart Reactor and Battery

The startup system consisted of a 2-MW_e, pellet bed nuclear fission reactor power system and a nickel hydrogen (NiH) bipolar battery bank. Weeks before departure, the startup reactor was used to refrigerate the TF/PF/divertor/magnetic nozzle coils gradually, initiate and ramp up their current, provide auxiliary power, and charge up the battery. When all systems and crew were ready, rf heating initiated plasma formation in the core of the fusion reactor. Then the final plasma startup sequence was executed with a ~6.5–10 s battery bank discharge providing ~1 GJ of energy (154 MW_e of input power) to the HHFW system. Together with fuel pellet injection, the reactor passed through breakeven and proceeded to ignition conditions.

Before current startup and HHFW heating to ignition conditions, ~1 MW of auxiliary rf heating at the electron cyclotron frequency was used to create a small volume of high-conductivity plasma ($T_e \sim 100$ eV and $n_e \sim 10^{19}/m^3$). During this "expanding radius startup,"[35] new layers of plasma were added to the warm core through ionization of a regulated gas feed. As the plasma minor radius grew in size, sufficiently high levels of current and plasma density were achieved to ensure adequate confinement of energetic protons from D^3He fusion. Heating to ignition conditions could then commence.

A small fission reactor was the heat source for a dynamic energy conversion system that supplied power during startup and emergency restart of the fusion reactor/propulsion system. During steady-state, interplanetary cruise, the fission reactor power system continued to supply auxiliary power. A high-temperature gas-cooled reactor (HTGR) of the pellet bed type[36] with a thermal power of ~6 MW_{th} was coupled to a regenerated CCGT power system. With a net thermal-to-electric conversion efficiency of >35%, it provided 2 MW_e of electrical power (Table 19).

The NiH bipolar batteries were derivatives of devices designed and tested, yielding 82% efficient, high peak power systems capable of specific energies of 180 kJ/kg and energy packaging densities of over 80 W · h/l (Ref. 37) (Table 20).

Should the fusion reactor need to be restarted during the interplanetary transit, the same startup sequence would be followed. The startup reactor power would also be used to maintain the refrigeration of critical systems. Should the battery bank fail to restart the fusion reactor, sufficient startup reactor power would be available to recharge the bank within 2 h.

Weight Growth Contingency

Weight growth contingency is the margin allocated to compensate for the inevitable growth in mass experienced by aerospace systems as designs mature and construction proceeds. Experience with the development of 18 major aerospace vehicles has demonstrated that

Table 19 Startup fission reactor and power system characteristics

Parameter	Design value
Reactor type	HTGR pellet bed
Thermal power, MW_{th}	6
Reactor volume, l	3
Radiation shielding, n, γ, solid angle	4π
Shielding material	Tungsten
Power cycle type	Regenerated CCGT
Electrical power, MW_e	2
Working fluid	GHe
Fluid temperature (hot), K	1,700
Fluid flow rate, kg/s	2.1
Cycle temperature ratio	3.6
Cycle pressure ratio	2.5
Power conversion efficiency, %	35.6
Turboalternator speed, rpm	36,000
ac frequency, Hz	600
Drive length, m	3
System diameter, m	0.7
Radiator surface area (two-sided), m^2	706
Total system mass, t	10

Table 20 Battery bank characteristics

Parameter	Design value
Battery type	NiH_2 bipolar
Specific energy, kJ/kg	180
Energy packing density, W · h/l	82.6
Discharge power (maximum), GW	1
Discharge time, s	6.5–10
Power conversion efficiency, %	82
Volume, m^3	3.36
Mass, t	5.6

from the point of initial contract proposal through the acquisition of the first unit, the total average weight growth experienced by military aerospace vehicles has been 25.5% (Ref. 38). For more than two dozen major inhabited and uninhabited vehicles/spacecraft (from the point of Phase C/D to first vehicle flight) most programs have experienced a similar 15–30% weight growth.[39,40] Given the immaturity of the majority of technologies used on the *Discovery II*, past aerospace experience suggests a prudent minimum value of 30% weight growth allowance be assessed on the total dry mass of the propulsion system and the crew payload. Thus, weight growth contingencies of 149 and 40 t were carried on the propulsion and payload systems, respectively, representing significant mass property contributions.

Conclusions

A conceptual vehicle system design predicated on a small-aspect-ratio spherical torus nuclear fusion reactor has the potential for enabling relatively fast outer solar system travel. The requirements for human missions to Jupiter were satisfied with a 172-t payload mass, a 1690-t IMLEO, and a 118-day one-way trip time. The vehicle concept provided high thrust (4000–6000 lbf), high I_{sp} (35,000–47,000 lbf s/lbm), and radial interplanetary transfers due to its high thrust-to-weight capability. In situ refueling capability was required for all round-trip missions. Design decisions were driven by the desire to maintain a balance between today's experimentally demonstrated technology and reasonable extrapolations to what might be available some 30 years from now.

Analysis, design, and assessment were performed on all major systems, including shielded/artificial gravity crew payload, central truss, nuclear fusion reactor, magnetic nozzle, power conversion (turbine, generator, radiator, and conditioning), HHFW heating, refrigeration, tankage, avionics, startup fission reactor and battery bank, fuel pellet injection, communications, reaction control systems, mission design, assembly, and space operations. Related experimental and theoretical efforts are currently underway. Overall feasibility of nuclear fusion propulsion systems must include assessments of related space infrastructure such as heavy lift launch

vehicles, space-based orbit transfer vehicles, and ISRU with associated cost of their operations. Many technical issues must be explored in depth before rendering judgment as to the practicality of a solar-system-class, nuclear-fusion-based transportation system for the 21st century.

Acknowledgments

The authors thank the many individuals from the following institutions who have provided essential guidance and expertise to this effort: Department of Energy (DOE) Princeton Plasma Physics Laboratory; DOE Los Alamos National Laboratory; The Ohio State University; University of Wisconsin; DOE Oak Ridge National Laboratory; NASA John H. Glenn Research Center at Lewis Field; DOE Idaho National Engineering Laboratory; Brush Wellman, Inc.; Westinghouse Science and Technology Center; The Boeing Company; DOE Sandia National Laboratories; NASA Ames Research Center; Primex Technologies Corp.; Analex Corp.; and NASA Langley Research Center.

References

[1]Williams, C. H., "Trajectory Design and Mission Analysis of Fast, Outer Solar System Travel," American Astronautical Association, Paper 01-161, Feb. 2001.

[2]Williams, C. H., Borowski, S. K., Dudzinski, L. A., and Juhasz, A. J., "A Spherical Torus Nuclear Fusion Reactor Space Propulsion Vehicle Concept for Fast Interplanetary Piloted and Robotic Missions," AIAA Paper 99-2704, June 1999.

[3]Williams, C. H., Borowski, S. K., Dudzinski, L. A., and Juhasz, A. J., "A Spherical Torus Nuclear Fusion Reactor Space Propulsion Vehicle Concept for Fast Interplanetary Travel," NASA TM 208831, Dec. 1998.

[4]Williams, C. H., and Borowski, S. K., "An Assessment of Space Propulsion Fusion Concepts and Desired Operating Parameters for Fast Solar System Travel," AIAA Paper 97-3074, July 1997.

[5]Williams, C. H., and Borowski, S. K., "Commercially-Driven Human Interplanetary Propulsion Systems: Rationale, Concept, Technology, and Performance Requirements," *13th Symposium on Space Nuclear Power and Propulsion*, Conf. Proceedings 361, American Inst. of Physics, Woodbury, NY, 1996, pp. 1057–1064.

[6]Williams, C. H., "An Analytic Approximation to Very High Specific Impulse and Specific Power Interplanetary Space Mission Analysis," NASA TM 107058, Sept. 1995.

[7]Williams, C. H., Dudzinski, L. A., Borowski, S. K., and Juhasz, A. J., "Realizing '2001: A Space Odyssey': Piloted Spherical Torus Nuclear Fusion Propulsion," AIAA Paper 2001-3805, July 2001.

[8]Borowski, S. K., "A Comparison of Fusion/Antiproton Propulsion Systems for Interplanetary Travel," AIAA Paper 87-1814, July 1987.

[9]Isakowitz, S. J., Hopkins, J. P., and Hopkins, J. B., *International Reference Guide to Space Launch Systems*, AIAA, Reston, VA, 1999, pp. 396, 407.

[10]Borowski, S. K., Dudzinski, L. A., and McGuire, M. L., "Artificial Gravity Vehicle Design Option for NASA's Human Mars Mission Using 'Bimodal' NTR Propulsion," AIAA Paper 99-2545, June 1999.

[11]Paloski, W. H., and Young, L. R., "1999 Artificial Gravity Workshop," *Proceedings and Recommendations*, League City, TX, Jan. 1999. pp. 44–54.

[12]Clark, B. C., "Concept 6: An Artificial Gravity Mars Spaceship," *Space Technology*, Vol. 11, No. 4, 1991, pp. 205–216.

[13]Wilson, J. W., Miller, J., Konradi, A., and Cucinotta, F. A., "Shielding Strategies for Human Space Exploration," NASA CP 3360, Dec. 1997.

[14]Stanford, M., and Jones, J. A., "Space Radiation Concerns for Manned Exploration," *Acta Astronautica*, Vol. 45, No. 1, 1999. pp. 39–47.

[15]Borowski, S. K., and Strickler, D. J., "Profile Effects and Plasma Power Balance," Oak Ridge National Lab., Paper Conf-8505175–1, Oak Ridge, TN, Dec. 1985.

[16]Mitarai, O., Hasuyama, H., and Wakuta, Y., "Spin Polarization Effect on Ignition Access Condition for D-T and D^3He Tokamak Fusion Reactors," *Fusion Technology*, Vol. 21, July 1992, pp. 2265–2283.

[17]Christiansen, J. P., Cordey, J. G., Thomsen, K., Tanga, A., DeBoo, J. C., and Schissel, D. P., "Global Energy Confinement H-Mode Database for ITER," *Nuclear Fusion*, Vol. 32, No. 2, 1992, pp. 291–338.

[18]Service, R. F., "New Superconductor Stands Up to Magnetic Fields," *Science*, Vol. 268, May 1995, p. 644.

[19]Awaji, S., Watanabe, K., and Kobayashi, N., "Crossover from Intrinsic to Extrinsic Pinning for $YBa_2Cu_3O_7$ Films," *Cryogenics*, Vol. 39, 1999, pp. 569–577.

[20]Boyer, R., Welsch, G., and Collings, E. W., *Materials Properties Handbook: Titanium Alloys*, American Society for Metals Handbook, ASM International, Materials Park, OH, 1994, pp. 68–72.

[21]Roth, J. R., *Introduction to Fusion Energy*, 4th ed., Ibis, Charlottesville, VA, 1988, pp. 299, 534–536.

[22]Baker, C. C., "Technology Implications of Advanced Fusion Fuel Cycles," *Proceedings of the 1979 IEEE International Conference on Plasma Science*, Inst. of Electrical and Electronics Engineers, New York, 1979, Paper 263, p. 50.

[23]Gerwin, R., "Summary Report on Plasma Propellant–Magnetic Nozzle Interface," Dept. of Energy Preprint, Los Alamos National Lab., Los Alamos, NM, April 1999.

[24]Cikanek, H. A., "Lewis Research Center Revised Submissions to the Advanced Technology Lead Center for the Fiscal Year 2000 Budget Call," NASA Official Letter, June 1998.

[25]Sankovic, J. M., Hamley, J. A., Haag, T. W., Sarmiento, C. J., and Curran, F. M., "Hydrogen Arcjet Technology," NASA TM 105340, Oct. 1991.

[26]Boehm, E., "High Temperature Reactors with Gas Turbines," *Atomkernenergie*, No. 11, 1966, pp. 343–352.

[27]Keller, C., and Schmidt, D., "Industrial Closed-Cycle Gas Turbines for Conventional and Nuclear Fuel," American Society of Mechanical Engineers, Publ. 67-GT-10, March 1967.

[28]Spitzer, J., Ono, M., Peng, M., Bashore, D., Bigelow, T., and Brooks, A., "Engineering Design of the National Spherical Tokamak Experiment," *Fusion Technology*, Vol. 30, Dec. 1996. pp. 1337–1342.

[29]Mau, T. K., Ehst, D. A., and Hoffman, D. J., "The Radio-Frequency Current-Drive System for the ARIES-I Tokamak Power Reactor," *Fusion Engineering and Design*, Vol. 24, 1994, pp. 205–227.

[30]"Nuclear Reactor/Propulsion System Interaction," Final Rept., NASA Contract NAS3-25972, Task 18, General Dynamics Space Systems Div., San Diego, CA, Nov. 1993.

[31]Glaister, D. S., Donabedian, M., Curran, D. G. T., and Davis, T., "An Assessment of the State of Cryocooler Technology for Space Applications," AIAA Paper 98-5203, 1998.

[32]Kittel, P., Salerno, L. J., and Plachta, D. W., "Cryocoolers for Human and Robotic Missions to Mars," *Cryocoolers*, Vol. 10, 1999, pp. 815–821.

[33]Drobyshevski, E. M., Zhukov, B. G., Kurakin, R. O., Sakharov, V. A., and Studenkov, A. M., "Electromagnetic Launch of MM-Size Pellets to Great Velocities," *Fusion Technology*, Vol. 26, Nov. 1994, pp. 649–653.

[34]Hawke, R. S., Nellis, W. J., Newman, G. H., Rego, J., and Susoeff, A. R., "Summary of EM Launcher Experiments Performed at LLNL," *IEEE Transactions on Magnetics*, Vol. MAG-22, No. 6, 1986, pp. 1510–1515.

[35]Borowski, S. K., "Inductive Current Startup in Large Tokamaks with Expanding Minor Radius and RF Assist," Oak Ridge National Lab., Rept. FEDC-83/8, Oak Ridge, TN, Feb. 1984.

[36]Juhasz, A. J., El-Genk, M. S., and Harper, W., "Closed Brayton Cycle Power System with a High Temperature Pellet Bed Reactor Heat Source for Nuclear–Electric Propulsion Applications," NASA TM 105933, Oct. 1992.

[37]Cataldo, R. L., "Test Results of a Ten Cell Bipolar Nickel–Hydrogen Battery," NASA TM 83384, Aug. 1983.

[38]Hawkins, K., "Space Vehicle and Associated Subsystem Weight Growth," Society of Allied Weight Engineers, Paper 1816, May 1988.

[39]Shelton, W., "MSFC Programs Weight Growth History," NASA Marshall Spaceflight Center, Huntsville, AL, April 1979.

[40]Walton, T. P., and Smith, R. E., "Weight Control and Weight Histories of Marshall Space Flight Center Projects," NASA MSFC-RPT-1553 A, July 1991.

J. A. Martin
Associate Editor